Arabian Journal of Chemistry (2023) **16**, 105009

King Saud University

Arabian Journal of Chemistry

www.ksu.edu.sa
www.sciencedirect.com

ORIGINAL ARTICLE

Aminophosphonic acid derivatized polyacrylonitrile fiber for rapid adsorption of $Au(S_2O_3)_2^{3-}$ from thiosulfate solution

Zhujuan Li, Shuliang Chen, Futing Zi *, Xianzhi Hu *, Yunlong Chen

Faculty of Science, Kunming University of Science and Technology, Kunming 650500, China

Received 8 February 2023; revised 12 May 2023; accepted 13 May 2023
Available online 19 May 2023

KEYWORDS

Polyacrylonitrile fibre;
Gold thiosulfate complex;
Recovery;
Chemical grafting

Abstract A fast and efficient Au (I) recovery adsorption method from an actual leaching solution of Cu^{2+}-en-$S_2O_3^{2-}$ is presented. Aminophosphonic acid derivatized polyacrylonitrile fibers (PAN-NP), prepared with triethylenetetramine and phosphoric acid by chemical grafting, were used as the adsorbent. The adsorbent was well characterized by FT-IR, SEM, TGA and XPS. The effects of contact time, pH, temperature, and Au (I) concentration were also investigated. PAN-NP can rapidly capture $Au(S_2O_3)_2^{3-}$ (20 min) and has a maximum adsorption capacity of 14.68 kg/t. Compared with -SH modified, PAN-NP has better stability and without oxidized. The adsorption process was described based on the Langmuir isothermal model (R^2 > 0.99). Thermodynamic parameters indicated that the adsorption of $Au(S_2O_3)_2^{3-}$ on PAN-NP was exothermic (ΔH^{θ} = −9.906 kJ/mol) and adsorption mechanism involved a collective effect resulting the anion exchange of $Au(S_2O_3)_2^{3-}$ with $-RNH_3^+H_2PO_3^-$, electrostatic attraction between $-RNH_3^+$ and $Au(S_2O_3)_2^{3-}$ and complexation of P = O with Au (I). Besides, PAN-NP-Au can be effectively eluted by sodium sulfite. Importantly, in the Cu^{2+}-en-$S_2O_3^{2-}$ actual leaching solution, the PAN-NP can efficiently recover Au (I) with an adsorption percentage of up to 97 % at a the solid-liquid ratio of 1:50, thereby affording a satisfactory application result. This is a meaningful method for recovering Au (I) from thiosulfate solution.

1. Introduction

Cyanidation is the predominant leaching method for gold. However, the cyanide is a highly toxic reagent that adversely impacts the human and environment health, it banned in many countries now (Dong et al., 2019; Wang et al., 2020; Yang et al., 2021). so, non-cyanide gold-leaching methods increasing attention. The thiosulfate method own to inexpensive, non-toxic, fast leaching rate, and good selectivity for gold, it is considered the most promising method for gold extraction (Jeon et al., 2020; Xu et al., 2019). Notably, utilization of Cu^{2+}–NH_3-$S_2O_3^{2-}$ and Cu^{2+}-en-$S_2O_3^{2-}$ complexes as catalytic oxidizers can

* Corresponding authors.
E-mail addresses: 345992103@qq.com (F. Zi), xianzhihu2@sina.com (X. Hu).

Peer review under responsibility of King Saud University. Production and hosting by Elsevier.

Production and hosting by Elsevier

https://doi.org/10.1016/j.arabjc.2023.105009
1878-5352

effectively promote the dissolution of gold (Wang et al., 2019). Despite these advantages, however, the application of this method is not used extensively in industries, because an acceptable and practical method for the recovery of Au (I) from pregnant thiosulfate solutions has still not been developed (Dong et al., 2021).

Several methods such as cementation (Hiskey and Lee, 2003), solvent extraction (Jin Zhao 1998), electrodeposition (Grosse et al., 2003), and adsorption (Wang et al., 2021) have been developed and used to recover Au (I) from thiosulfate leaching pregnant solutions. Gold in thiosulfate solution can be better cemented using zinc and aluminum; however, this method has difficulty in solid–liquid separation and with high economic cost. Solvent extraction is suitable for solutions with high gold concentration; however, the actual leaching solution has low gold concentration. Multiple side reactions and high consumption of reagents reduce the gold purity during the electrodeposition process. Adsorption is the most advantageous because of its availability, inexpensive reagents, facile operation, and easy regeneration (Dong et al., 2017). Adsorbents such as activated carbon (Jiang et al., 2022), resins (Zhang et al., 2021b), and silica gel (Chen et al., 2020a) have been used to recover Au (I) and fruitful advancements have been reported. However, activated carbon has very weak affinity to Au (I) (Jiang et al., 2022), therefore, Chen and Wang modified activated carbon and reported significantly enhanced adsorption capability of Au (I). However, they reported the adsorption of Au (I) in pure thiosulfate solution only, which had poor anti-interference abilities (Chen et al., 2020b; Wang et al., 2020). Plsniak recovered Au (I) from ammonium thiosulfate solutions using a synthetic polymer resin and reported satisfactory results (Pilśniak et al., 2009). Lack of selectivity, high material costs, easy pulverization, and poisoning (blocked apertures) hamper the development of resins. Chen investigated the performance of mercapto-modified silica gel for Au (I) recovery in thiosulfate solution with reduced costs and a simplified modified process. However, the research on more complex systems has not been conducted yet, and the technology is not yet mature (Chen et al., 2020a). In addition, the -SH as modified group in above studies, but the -SH group is unstable and easily oxidized. Hence, for recovery of Au (I) from thiosulfate solutions effectively, it is essential to find new materials to fabricate adsorbents that exhibit excellent stability performance.

In recent years, textile fibers, a class of organic synthetic polymers, have been attracting increasing attention because of their excellent properties (Xiao et al., 2020). Such as cotton and polyacrylonitrile (PAN) fibers (Zhao et al., 2017). PAN fibers are one of the most promising textile fibers (Zhang et al., 2022). They are environmentally friendly material and are widely used in industry and daily life. Furthermore, they can be easily woven into various shapes in flow processes (Du et al., 2016). They are inexpensive and resistant to corrosion and mildew attack and have a simple production process, high strength, low density, ease of modification (Shi et al., 2016). They contain abundant cyano groups, which can be easily transformed into various functionalities (such as carboxyl, amide, and amidoxime) through chemical reactions (Li et al., 2011). For instance, removal of Hg (II) from wastewater has been reported using modified PAN (Nasimi et al., 2020). However, use of PAN as an adsorbent to recover Au (I) from thiosulfate solution have not reported. Aminophosphonic acid containing amino and phosphoric acid groups is an effective chelating ligand for many metal ions. Therefore, it is necessary to develop a more selective and reusable functionalized PAN for practical application.

A novel aminophosphonic acid-derivatized polyacrylonitrile fiber (PAN-NP) as an Au (I) adsorbent from thiosulfate solution is reported in this study. Compared with -SH, aminophosphonic acid modified has better stability, it is not oxidized placed in the air for a long time. Therefore, the adsorption material with good stability is prepared by the modification way. It provides theoretical support for gold recovery and has great significance. To the best of our knowledge, this is the first report on the use of PAN-NP to recover Au (I) from thiosulfate solution. Additionally, the adsorption performance, characterization, adsorption mechanism, and recovery performance in the actual mines of PAN-NP for Au (I) in Cu^{2+}-en-$S_2O_3^{2-}$ solution are studied. Due to the nature of the material itself, it can be predicted that it can achieve a better separation effect in the actual slurry. In sum, the method is meaningful for development of recovery Au (I) from thiosulfate solution.

2. Experimental

2.1. Materials

2.1.1. Reagents

Commercially available PAN (93.0 % acrylonitrile, 6.5 % methyl acrylate and 0.4–0.5 % sodium styrene sulfonate, from the Fushun Petrochemical Corporation of China) was cut into the lengths about 1 cm before used. Triethylene tetramine (TETA, 65 %), H_3PO_3 (99 %), sodium thiosulfate ($Na_2S_2O_3$), gold powder (99.99 % from Sino Platinum Metals Corp, Guizhou, China), Formaldehyde (40 %), ethylenediamine (en, 99 %), and cupric sulfate ($CuSO_4{\cdot}5H_2O$) were obtained from the Shanghai Aladdin Industrial Company. All the reagents were of analytical grade. Deionized water was used.

2.2. Methods

2.2.1. Synthesis of PAN-NP

The synthesis of PAN-NP was carried out in two stages (Scheme 1). The amine-functionalized fiber (PAN-N) was fabricated using previously reported methods (Xu et al., 2018). Firstly, dried PAN (5 g), triethylene tetramine (100 mL), and deionized water (50 mL) were added to a round-bottomed flask (250 mL). Next, the mixtures were refluxed and stirred at 140 °C for 4 h. They were then taken out and washed to neutrality with hot water (60–70 °C) using a suction filter device. The washed fiber was dried in a vacuum oven at 60 °C for 12 h to obtain the PAN-N. Secondly, dried PAN-N (5 g), solid phosphorous acid (25 g), 40 % formaldehyde (50 mL), and absolute ethanol (125 mL) were added to another round-bottomed flask (250 mL). The mixture was stirred and refluxed at 80 °C for 4 h, the reactants taken out, and the solution was washed to neutrality with deionized water and absolute ethanol using a suction filter device. The fiber was then dried overnight in a vacuum oven at 60 °C to obtain PAN-NP. The optimization of PAN-NP was demonstrated in the supplementary information.

The extent of the fiber was derivatized was described based on the weight gain using the following equation. *Weight gain* $S = \frac{W_2 - W_1}{W_1} \times 100$, where W_1 and W_2 are, respectively, the weights of PAN and PAN-N at the amination stage. For the phosphonic acid-grafting stage, W_1 and W_2 are the weights of PAN and PAN-NP, respectively.

2.2.2. Preparation of $Au(S_2O_3)_2^{3-}$ complex

The prepare of $Au(S_2O_3)_2^{3-}$ adsorption solution was conducted based on the previously reported methods (Yu et al., 2015). First, a certain amount of gold powder was added into the aqua regia solution and heated to dissolve. Then, a few drops of 10 % KCl were mixed with it and the resulting solution was heated to nearly dryness. Next, an appropriate weight of sodium thiosulfate was mixed with them to obtain the Au $(S_2O_3)_2^{3-}$ solution. Prior to conducting adsorption experiments, the pH of $Au(S_2O_3)_2^{3-}$ was adjusted to 9.0 with 0.1 mol/L of

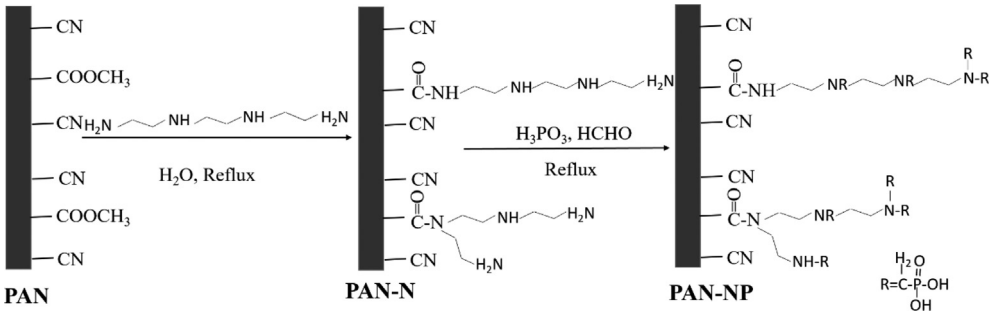

Scheme 1 Schematic diagram of the synthesis of PAN.

NaOH and 0.1 mol/L of HCl. The concentration of Au $(S_2O_3)_2^{3-}$ required for the experiment was obtained by dilution.

2.2.3. Preparation Cu^{2+}-en-$S_2O_3^{2-}$ solution

The Cu^{2+}-en-$S_2O_3^{2-}$ solution was prepared according to a previously reported method (Wang et al., 2019), Here, 5 mmol/L of Cu^{2+} was used. The molar ratio of Cu^{2+}/en was fixed at 1:2. The prepared $Na_2S_2O_3$ solution was added to the Cu^{2+}-en solution, and the volume was increased to 100 mL using a leaching solution. This solution was then used for conducting the adsorption experiment (Section 2.3).

2.3. Adsorption experiment

The adsorption performance of $Au(S_2O_3)_2^{3-}$ on PAN-NP was investigated next. First, 0.5 g of PAN-NP was added to 100 mL of $Au(S_2O_3)_2^{3-}$ to achieve 0.1 mol/L of sodium thiosulfate solution (the initial gold concentration was 50 mg/L). This solution was then added to a 250 mL Erlenmeyer flask. The mixture was stirred at 220 rpm at the room temperature for a certain period. A portion of the adsorption solution (5 mL) was then analyzed to determine the Au (I) concentration. Besides, to reduce the experimental data error as much as possible, the experimental samples were investigated in parallel. The adsorption percentage (R) (Eq. (1)) and loading capacity (Q) (Eq. (2)) were used to estimate the adsorption performance of $Au(S_2O_3)_2^{3-}$ on PAN-NP.

$$R = \frac{c_0 v_0 - c_t v_t}{c_0 v_0} \times 100\% \quad (1)$$

$$Q = \frac{c_0 v_0 - c_t v_t}{M} \quad (2)$$

R is the adsorption percentage of $Au(S_2O_3)_2^{3-}$ on PAN-NP, c_0 is the initial concentration of Au (I), v_0 is the initial volume of thiosulfate solution, and c_t and v_t are the Au (I) concentration and volume at a given time, respectively. Q (mg. g^{-1}) is the loading capacity of Au (I) on PAN-NP and M (g) is the weight of the adsorbent used.

2.4. Material characterization

The Au (I) concentration was analyzed by the AAS (AAS-300, PerkinElmer, USA). The KBr pellet method was to analyze the construction of all fibers. The FT-IR (wavenumber range of 4000–400 cm^{-1}) (Nicolet iS10, Thermo Fisher, Waltham, MA, USA) and the SEM-EDS (Phenom Prox, FEI Co., USA) were employed to explore material characteristics. The XPS (PHI 5500, Versaprobe-II, USA) was also employed to distinguish the elemental chemical valence environment of the fibers. The XPS data were analyzed using Avantage Software. The C 1 s spectrum at 284.8 eV was used to calibrate the internal standard for charge compensation. The TGA was employed to inspect the thermal stability of the adsorbent (STA, 499C, Germany).

3. Results and discussion

3.1. Synthesis of the PAN-NP

The level of amination reaction is greatly affected by reaction time, reaction temperature, and amine concentration (Li et al., 2012). The weight gain was greatly affected by both too long reaction times and too high reaction temperatures, which notably reduces the mechanical strength of the PAN-NP. Combined with the optimization experiments and parameters such as specific surface area of the adsorbent, the 25.5 % weight gained of PAN-N based on PAN and the 39.9 % weight gained of PAN-NP based on PAN were selected to evaluate the extent of derivatization of PAN-NP and to conduct the subsequent experiments. PAN-NP-Au was used to represent the adsorbent after the adsorption.

3.2. Material characterization

3.2.1. FT-IR

The FT-IR spectra of PAN, PAN-N, PAN-NP, and PAN-NP-Au are illustrated in Fig. 1. The characteristic peaks of PAN were observed at 2245 and 1735 cm^{-1}, owing to stretching vibrations of C≡N and C = O, respectively (Fig. 1(a)) (Xu et al., 2016). After amination, an absorption peak (Fig. 1(b)) appeared at 3120 cm^{-1}, which was attributed to the stretching vibration of the N–H group. It indicates that the amino group was successfully derivatized on PAN and amino-active sites were generated. In addition, the C = O stretching vibration peak of PAN-N red-shifted from 1735 to 1662 cm^{-1}; in contrast, the C≡N peak did not change significantly after amination. Hence, compared to the nitrile groups, the ester groups are more likely to undergo aminolysis to form an amide bond during the derivatization on the surface layers. New adsorption peaks are generated at 1168 and 916 cm^{-1}, which can be attributed to the stretching vibration peaks of P = O and P–O, respectively (Fig. 1(c)) (Ma and Qiao, 2014). It demonstrates that the phosphonic acid is derivatized on the PAN-N

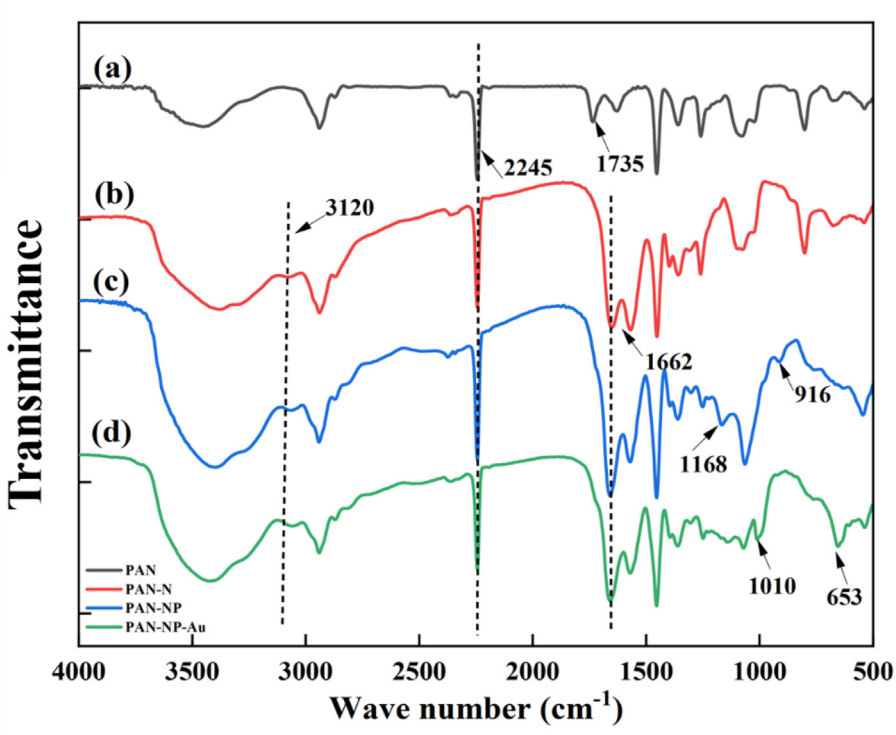

Fig. 1 The FT-IR spectra of PAN (a), PAN-N (b), PAN-NP (c) and PAN-NP-Au (d).

successfully. PAN-NP-Au showed two new absorption peaks at 1010 and 653 cm^{-1}, which are assigned to the characteristic peak of S = O and S–O, respectively, and were attributed to $S_2O_3^{2-}$ adsorption ((Fig. 1(d))) (Jeon et al., 2018; Watling, 2006). It shows that the derivatization was successful.

3.2.2. SEM studies

The SEM images of PAN, PAN-N, PAN-NP and PAN-NP-Au are presented in Fig. 2. The low-resolution SEM image demonstrates that all fibers have continuous surfaces with well-maintained integrity. Hence, it is suggested that the fiber structure was almost undamaged by the derivatization reaction. The original PAN has a smooth and uniform surface (Fig. 2 a, 2000 ×). The diameter of the fiber increased after amination and phosphonic grafting owing to the swelling effect (Fig. 2(b-c)). Many crack structures were found on the fiber surface. These structures provide a wider contact area for the adsorption of $Au(S_2O_3)_2^{3-}$ on the PAN-NP surface to allow more quick and facile adsorption. The adsorption did not cause any significant changes on the surfaces and integrity of the fibers (Fig. 2 d), indicating that PAN-NP is durable and should be recyclable. The EDS spectrum also illustrates successful derivatization of aminophosphonic acid on the PAN. As expected, the result is basically consistent with those of FT-IR.

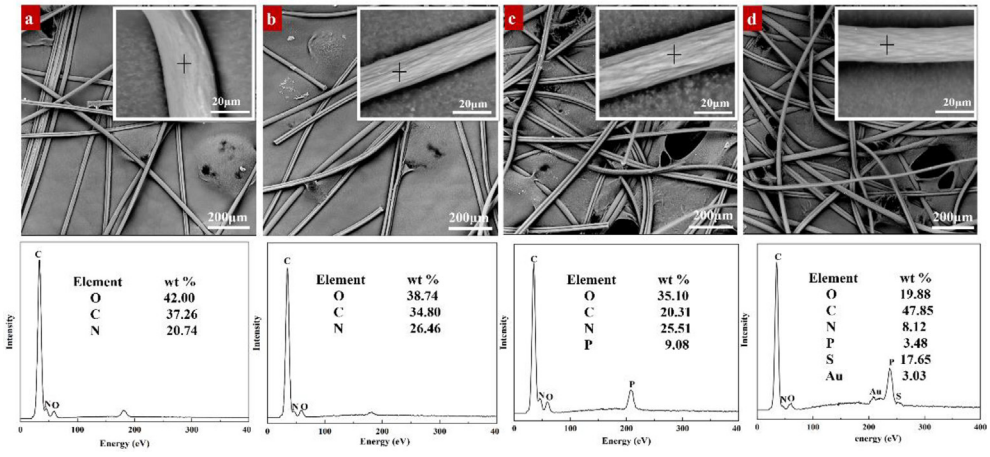

Fig. 2 The SEM images and EDS analysis. (a: PAN, b: PAN-N, c: PAN-NP, and d: PAN-NP-Au).

3.2.3. TGA studies

The thermal stability of the fibers was studied. The thermograms were recorded from 30 to 800 ℃ at a heating rate of 10 ℃ min^{-1} under nitrogen atmosphere, as shown in Fig. 3. The TGA curve of the original PAN clearly shows an initial decomposition temperature of 315 °C (Zhu et al., 2019). After derivatization and adsorption, PAN-N, PAN-NP, and PAN-NP-Au began to decompose when the temperature was reduced from 315 to 245 °C. Moreover, the decomposition of all fibers comprises four stages. Before 200 °C, the loss of moisture mainly occurs. Between 245 °C and 320 °C, the decomposition is attributed to the weight loss caused by the cleavage of the C–N bond (Seydibeyoğlu, 2012). Similarly, the weight loss at 320–500 °C can be attributed to the cleavage of C–C bond (Rahaman et al., 2007). Loss of non-carbon elements and finally the formation of gas occur between 500 and 800 °C. In brief, although the temperature at which the derivatized fiber show weight loss is lesser than that of the original PAN, it is sufficient to use it with a series of derivatized reactions. Hence, it is suggested that the PAN has a good thermal stability.

3.3. Adsorption experiment

3.3.1. The adsorption properties of PAN and PAN-NP

It is observed from Fig. 4, the adsorption percentage of Au (Ⅰ) in thiosulfate solution by PAN is about 8 % when adsorption for 20 min, while that by PAN-NP reached 59.9 %. The adsorption performance of PAN-NP for Au (Ⅰ) is different from lightly that of modified silica for Au (Ⅰ) in thiosulfate solution (Chen et al., 2020a). It is seen that by chemical grafting, the adsorption percentage of Au (Ⅰ) in $Au(S_2O_3)_2^{3-}$ solution is significantly improved. Therefore, it is feasible to recover Au (Ⅰ) from thiosulfate solution by chemical grafting of amino phosphonic acid onto PAN surface.

3.3.2. Effects of initial pH

The effect of pH on the recovery percentage was studied by varying the pH from 5 to 11 (Fig. 5). The adsorption percentage of $Au(S_2O_3)_2^{3-}$ on PAN-NP is only slightly affected by different initial pH values. When the pH is 5–7, the adsorbent shows a protonation effect, therefore, RNH_3^+ forms as the pH increases after adsorption. At pH 8–11, the deprotonation effect of the adsorbent reduces the pH. Finally, the pH was kept at 7.0. Previous studies have demonstrated that in the Cu^{2+}-en-$S_2O_3^{2-}$ gold leaching system, the optimum pH of pregnant thiosulfate leaching solution should be 9.0. (Wang et al., 2019). Hence, the pH 9.0 were also selected for further investigations. The PAN-NP has a wide range of pH application, which has great advantages in adsorptian was shown in the experiment.

3.3.3. Effects of contact time and multiple adsorption

The effect of contact time on the adsorption percentage was investigated. $Au(S_2O_3)_2^{3-}$ was extremely quickly adsorbed by PAN-NP (Fig. 6). Within the first 5 min, the adsorption percentage significantly increased and reached the equilibrium at 20 min. The adsorption percentage was 59.98% and the adsorption capacity was 5.81 kg/t. To completely recover Au $(S_2O_3)_2^{3-}$, the second adsorbent of the same weight was used to adsorb the remaining solution. We noted that 99.5% of $Au(S_2O_3)_2^{3-}$ could be absorbed after conducting the adsorption twice, indicating that $Au(S_2O_3)_2^{3-}$ can be completely recovered by PAN-NP. The adsorption behavior could be attributed to a

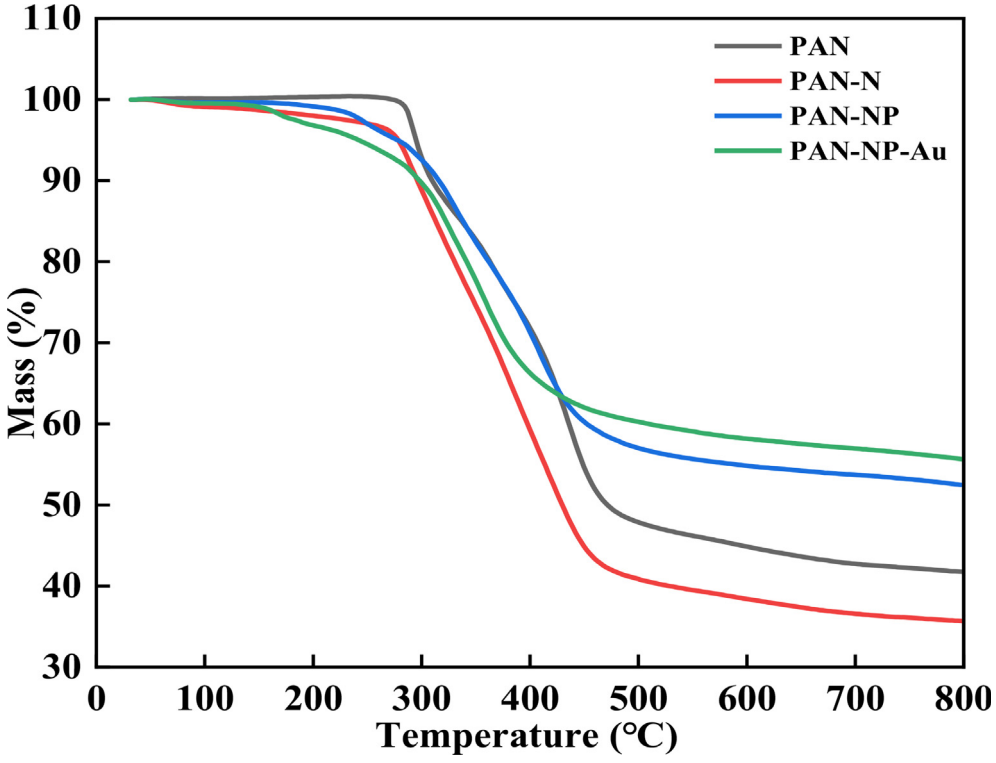

Fig. 3 The TGA of PAN, PAN-N, PAN-NP and PAN-NP-Au.

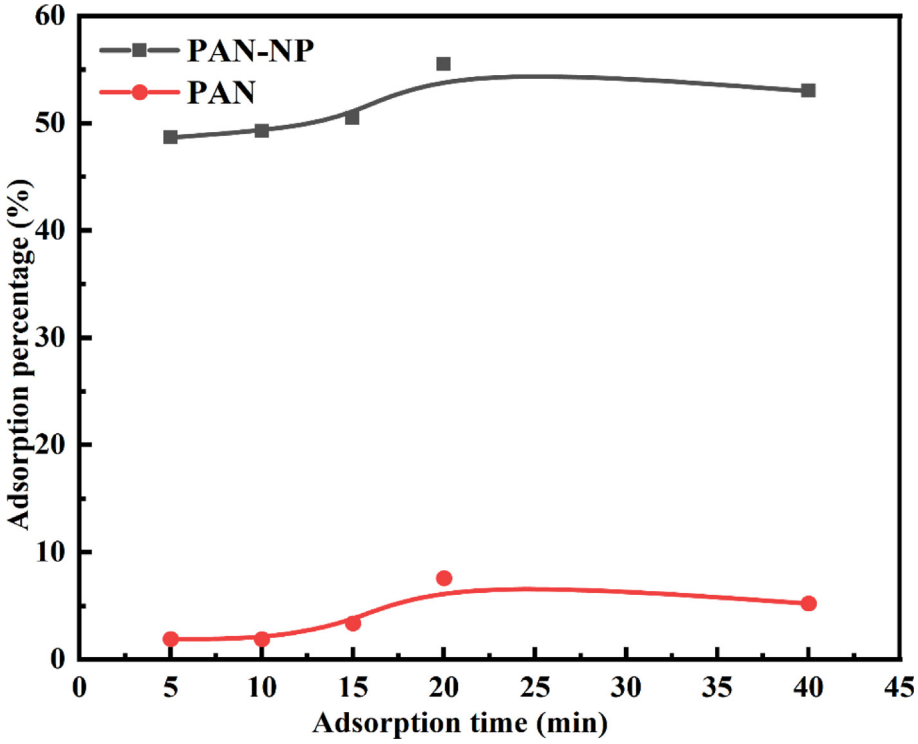

Fig. 4 The comparison of adsorption properties of PAN fibers before and after modification (m $_{PAN-NP}$ = 0.5 g; C Au^{+} = 50 mg/L; T = 25 °C; C $Na_2S_2O_3$ = 0.1 mol/L; pH = 9.0).

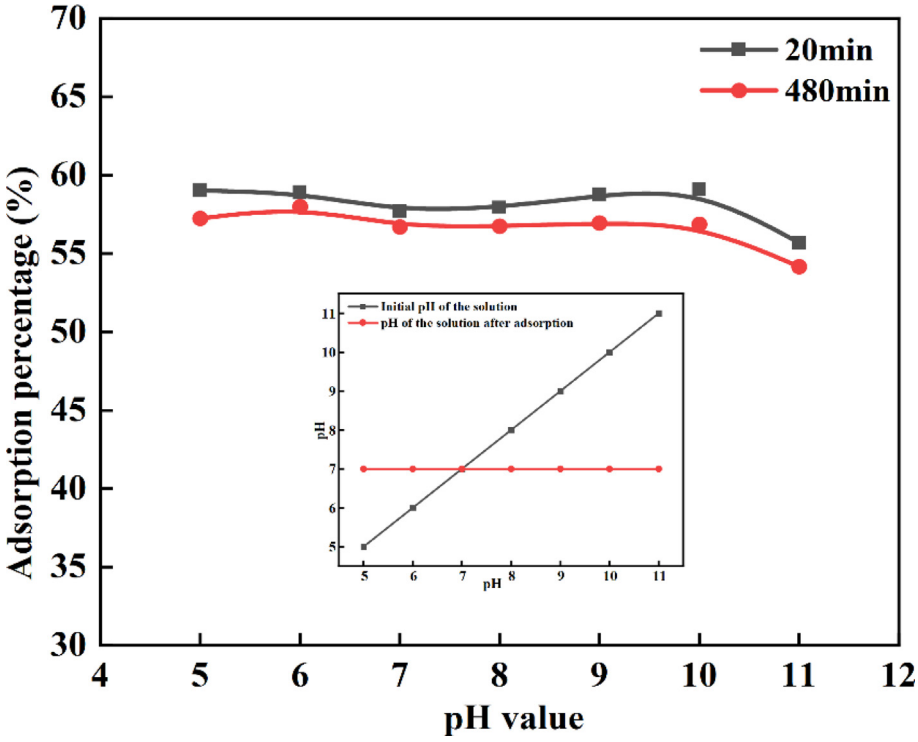

Fig. 5 Effect of pH on $Au(S_2O_3)_2^{3-}$ adsorption percentage. (m $_{PAN-NP}$ = 0.5 g; C $_{Au+}$ = 50 mg/L; T = 25 °C; C $_{Na2S2O3}$ = 0.1 mol/L).

reduction in the number of active sites of PAN-NP and a decrease in the Au (I) concentration. In addition, the trend of pH change after adsorption equilibrium is consistent with the effect of the pH value. When the PAN-NP was used for adsorption experiment after one month, it still had good adsorption performance (Fig. 6), indicating that PAN-NP

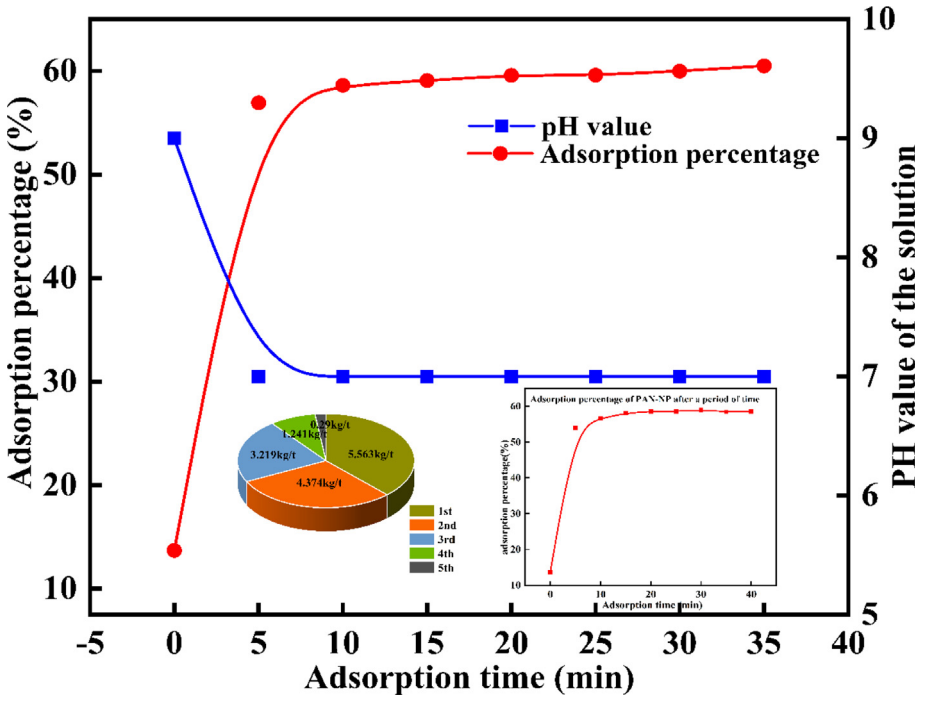

Fig. 6 $Au(S_2O_3)_2^{3-}$ adsorption equilibrium time and multistage adsorption on PAN-NP ($m_{PAN\text{-}NP}$ = 0.5 g; C_{Au+} = 50 mg/L; pH = 9.0; T = 25 °C; $C_{Na2S2O3}$ = 0.1 mol/L).

had excellent stability, this is consistent with the previous presentation.

The cumulative adsorption test was conducted next. After the first adsorption equilibrium, the adsorbent was transferred to another 100 mL of the same adsorption solution and five consecutive adsorptions were performed, the gold (I) adsorption capacity decreases with number of adsorption times, but still maintained at 0.29 kg/t at the fifth adsorption and the cumulative adsorption capacity became 14.68 kg/t (Fig. 6). Hence, PAN-NP can be used as an effective adsorbent, which is of great significance for the adsorption of Au (I) in thiosulfate solution.

3.3.4. *Effects of thiosulfate and initial Au (I) concentration*

We used a thiosulfate concentration of 0.01–0.4 mol/L for the experiments. The adsorption percentage tends to decrease with increasing thiosulfate concentration (Fig. 7(a)), owing to the $(S_2O_3)_2^{3-}$ anion interference. Following Au (I) concentrations were selected to investigate the effect on the adsorption behavior: 10, 15, 20, 30, 40, and 50 mg/L. The adsorption percentage decreases with increasing initial Au (I) concentration, which can be attributed to the limited number of active adsorption sites on the PAN-NP surface (Fig. 7(b)). At lower gold (I) concentrations, the adsorption percentage of $Au(S_2O_3)_2^{3-}$ is > 96 %.

3.3.5. *Effects of temperature on adsorption and adsorption thermodynamics*

To observe the effects of temperature on $Au(S_2O_3)_2^{3-}$ adsorption, we selected the 25, 35, 45, 55, and 65 °C to observed that the adsorption percentage decreases with increasing temperature (Fig. 8(a))). It is suggested that the adsorption of Au

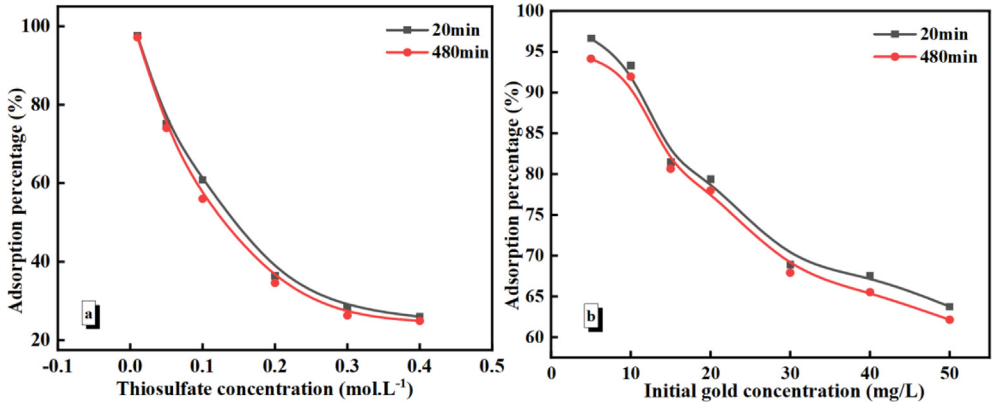

Fig. 7 Effect of thiosulfate concentration (a) and initial gold (I) concentration (b) for $Au(S_2O_3)_2^{3-}$ adsorption. ($m_{PAN\text{-}NP}$ = 0.5 g; pH = 9.0; T = 25 °C; C_{Au+} = 50 mg/L (a)/ $C_{Na2S2O3}$ = 0.1 mol/L (b)).

$(S_2O_3)_2^{3-}$ on the PAN-NP surface could be an exothermic process.

To observe the adsorption thermodynamics of $Au(S_2O_3)_2^{3-}$, the adsorption was conducted at 25, 35, 45, 55, and 65 °C. The various thermodynamic parameters were calculated using Eqs. (3)– (5) (Feng et al., 2018):

$$K_c = \frac{Q_e}{C_e} \tag{3}$$

$$\Delta G^{\theta} = \Delta H^{\theta} - T\Delta S^{\theta} \tag{4}$$

$$ln^{K_c} = \frac{\Delta S^{\theta}}{R} - \frac{\Delta H^{\theta}}{R}\frac{1}{T} \tag{5}$$

K_c is the equilibrium constant, C_e (mg L^{-1}) and Q_e (mg g^{-1}) are the equilibrium concentration and equilibrium adsorption capacity of Au (Ⅰ), respectively, T (K) is the adsorption temperature, and R (8.314 J·mol^{-1}·K^{-1}) is the ideal gas constant. ΔH^{θ} and ΔS^{θ} can be obtained separately from the intercept and slope of $\ln^{kc}$ and $1/T$ graphs. ΔG^{θ} values can be calculated from Eq. (4). The thermodynamic parameters of ΔS^{θ}, ΔG^{θ}, and ΔH^{θ} are shown in Table 1 at different temperatures. Table 1 also shows that ΔG^{θ} increases with increasing temperature. Hence, a high temperature is disadvantageous to the adsorption of $Au(S_2O_3)_2^{3-}$. This result also indicates that adsorption is an exothermic reaction due to negative value of the ΔH^{θ} (-9.906 KJ/mol) and the negative value of ΔS^{θ} suggested that the entropy of the system decreased upon adsorption (Zhang et al., 2019).

3.3.6. Adsorption isotherms

To understand the interaction between $Au(S_2O_3)_2^{3-}$ and PAN-NP, the adsorption isotherm was obtained at 308, 318, and 328 K meanwhile changing Au (Ⅰ) concentration at 10, 20, 30, 40, 50 and 60 mg/L were also observed. The adsorption isotherm data were fitted by Langmuir (Wu et al., 2019) and Freundlich isotherm models (Li et al., 2016) (Eqs. (6) and (7), respectively):

$$Langmuirmodel\frac{C_e}{q_e} = \frac{C_e}{q_m} + \frac{1}{q_m b} \tag{6}$$

$$Freundlichmodel q_e = kC_e^{1/n} \tag{7}$$

where q_e and q_{max} are the equilibrium adsorption capacity and maximum adsorption capacity of $Au(S_2O_3)_2^{3-}$ on PAN-NP, respectively; c_e is the Au (Ⅰ) concentration at adsorption equilibrium; K and b are the constants for Langmuir and Freundlich isotherm models, respectively; and n is the coefficient of the Freundlich isotherm model.

Linear plots obtained using $1/C_e$ vs $1/Q_e$ and ln $^{(ce)}$ vs ln $^{(qe)}$ are shown Fig. 9(a, b), respectively. The values of (q_{max}, b) and (k, n) can be determined from the slopes and intercepts of ($1/Q_e$ vs $1/C_e$) and (ln $^{(ce)}$ vs ln $^{(qe)}$) plots, respectively (Table 2). The Langmuir isotherm model ($R^2 > 0.99$) fitted to the experimental data of $Au(S_2O_3)_2^{3-}$ adsorption has a higher correlation coefficient than that of the Freundlich isotherm model ($R^2 > 0.94$). It indicates that the adsorption of Au $(S_2O_3)_2^{3-}$ on PAN-NP is a single-molecule chemisorption process. In addition, the n values were > 1, which suggests that $Au(S_2O_3)_2^{3-}$ could be easily adsorbed on PAN-NP under the experimental conditions.

3.3.7. Adsorption mechanism

XPS (Fig. 10), SEM, and FT-IR were used to investigate the adsorption mechanism of $Au(S_2O_3)_2^{3-}$ on PAN-NP. PAN-NP and PAN-NP-Au are made of C, O, and N elements (Fig. 10 (A)). Beside, new peaks of Au and S (Fig. 10(B,G)) (Ghahremaninezhad et al., 2013; Ma et al., 2020) were generated in the XPS fine spectrum of PAN-NP-Au. The fitting shows that gold peak observed under the chemical environment is that of Au (Ⅰ). Similarly, the fitting of the S peak shows that the sulfur occurs in the forms of S (Ⅱ) and S (Ⅵ), it is consistent with those obtained using FT-IR, so, the adsorption probably occurs between $Au(S_2O_3)_2^{3-}$ and PAN-NP.

Three types of nitrogen (Fig. 10(C)) are present in the XPS spectrum of PAN-NP: O = CN (401.77 eV), primary amine –RNH_2 (399.68 eV), and secondary amine –R_2NH (399.10 eV) (Luo et al., 2014; Xin-Gui Li, 2005; Zhang et al., 2017). After adsorption, the binding energies of –RNH_2 and –R_2NH (Fig. 10(D)) in the N1s spectrum shifted to higher values (400.20 and 399.62 eV, respectively) (Xin-Gui Li, 2020, 2019). The phenomenon was explained as follows: The N atom obtains electrons from the adsorption solution and undergoes a protonation reaction, and in the process, it gets converted to –RNH_3^+. Additionally, the P 2p fine spectrum of PAN-NP can be decomposed into two components: $H_2PO_3^-$ (133.08 and

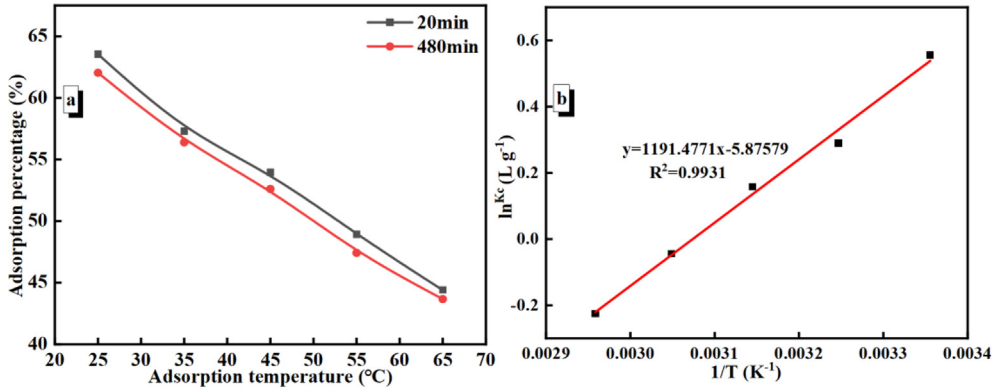

Fig. 8 Effect of temperature for $Au(S_2O_3)_2^{3-}$ adsorption (a) and Plot of ln Kc versus 1/T for the adsorption of $Au(S_2O_3)_2^{3-}$ on PAN-NP (b) (m_{PAN-NP} = 0.5 g; C_{Au+} = 50 mg/L; pH = 9.0; $C_{Na2S2O3}$ = 0.1 mol/L).

Table 1 $Au(S_2O_3)_2^{3-}$ complex thermodynamic parameters adsorbed on PAN-NP surface.

Temperature (K)	Kc	ΔG^0 ($kJ\ mol^{-1}$)	ΔH^0 ($kJ\ mol^{-1}$)	ΔS^0 ($J\ (mol.K)^{-1}$)
298	1.744	4.651	−9.906	−48.85
308	1.336	5.140	—	—
318	1.171	5.628	—	—
328	0.957	6.117	—	—
338	0.798	6.605	—	—

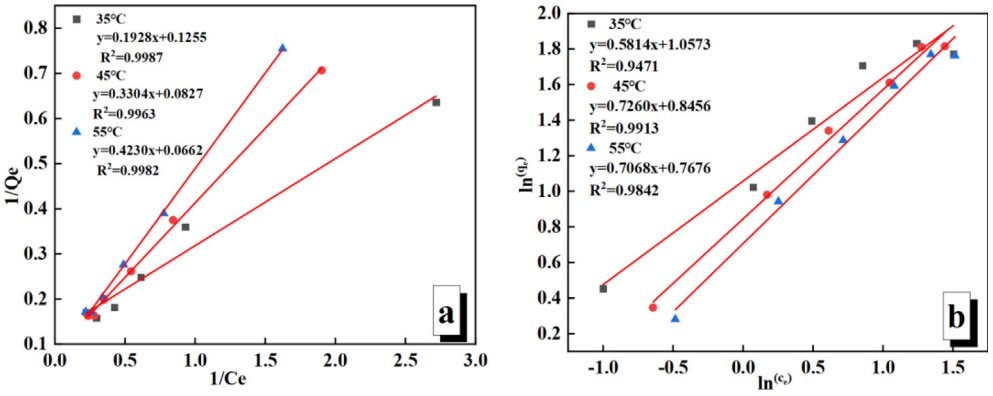

Fig. 9 Fits to Langmuir (a) and Freundlich (b) adsorption isotherm model for $Au(S_2O_3)_2^{3-}$ adsorption on PAN-NP.

Table 2 Parameters of the adsorption isotherm model (the units are listed in text).

Temperature (K)	Langmuir			Freundlich		
	R^2	b	q_m (mg/g)	R^2	n	k
308	0.9987	0.6510	7.968	0.9471	1.7199	2.8786
318	0.9963	0.2503	12.09	0.9913	1.3774	2.3294
328	0.9982	0.1560	15.10	0.9842	1.4148	2.1546

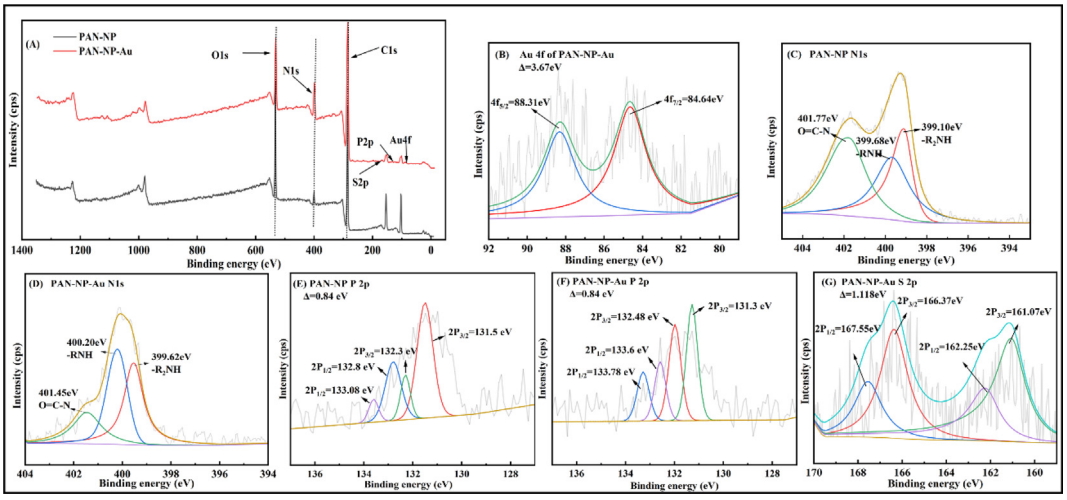

Fig. 10 XPS survey spectra of PAN-NP and PAN-NP-Au (A), Au 4f spectrum (B), N 1 s spectrum (C) (D), P 2p spectrum (E) (F), S 2p spectrum (G).

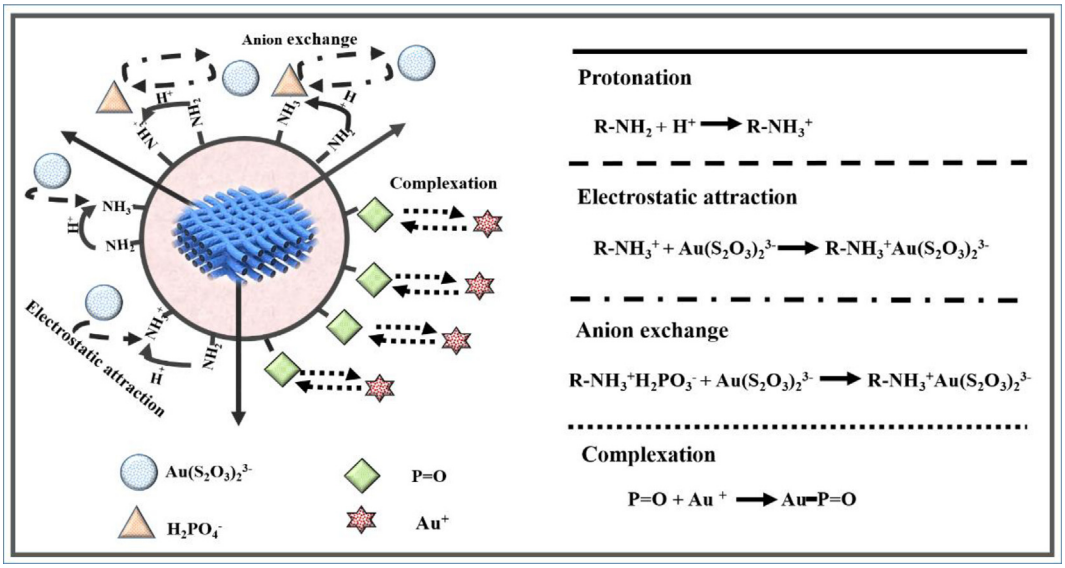

Fig. 11 Scheme for the mechanisms of $Au(S_2O_3)_2^{3-}$ adsorption by PAN-NP.

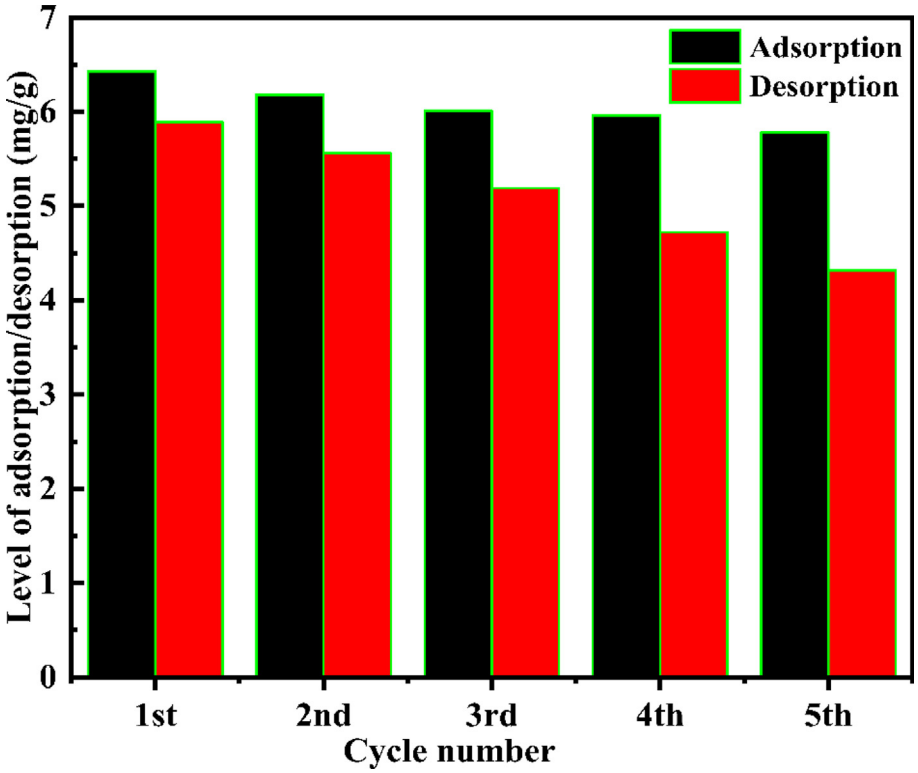

Fig. 12 Elution and reuse performance of PAN-NP.

132.3 eV) (Ren et al., 2016), and $H_2PO_4^-$ (132.8 and 131.5 eV) (Fig. 10 (E). The binding energy of $H_2PO_4^-$ after adsorption (Fig. 10 (F)) shifted to higher values (133.6 and 131.3 eV) (Zhang et al., 2021a), owing to complexation between Au (I) and the P = O group. Finally, the structure of Au. . . . . P = O is formed. Furthermore, the binding energy of $H_2PO_3^-$ slightly changes before and after the adsorption (133.78 and 132.48 eV, respectively). This phenomenon was observed because RNH_3^+ in PAN-NP is protonated and changes to $-RNH_3^+H_2PO_3^-$. During the adsorption, the protonated ammonia undergoes anion exchange between $Au(S_2O_3)_2^{3-}$ and $H_2PO_3^-$ during the adsorption of entire $Au(S_2O_3)_2^{3-}$. The electron binding energy of O = C–N does not change significantly after adsorption (401.45 eV), which also shows that O = C–N may not participate in the adsorption process. The protonation reaction of the N atom results in a positive charge; therefore, negatively charged groups can be attracted to it. Electrostatic attraction occurs between $-RNH_3^+$ and $Au(S_2O_3)_2^{3-}$.

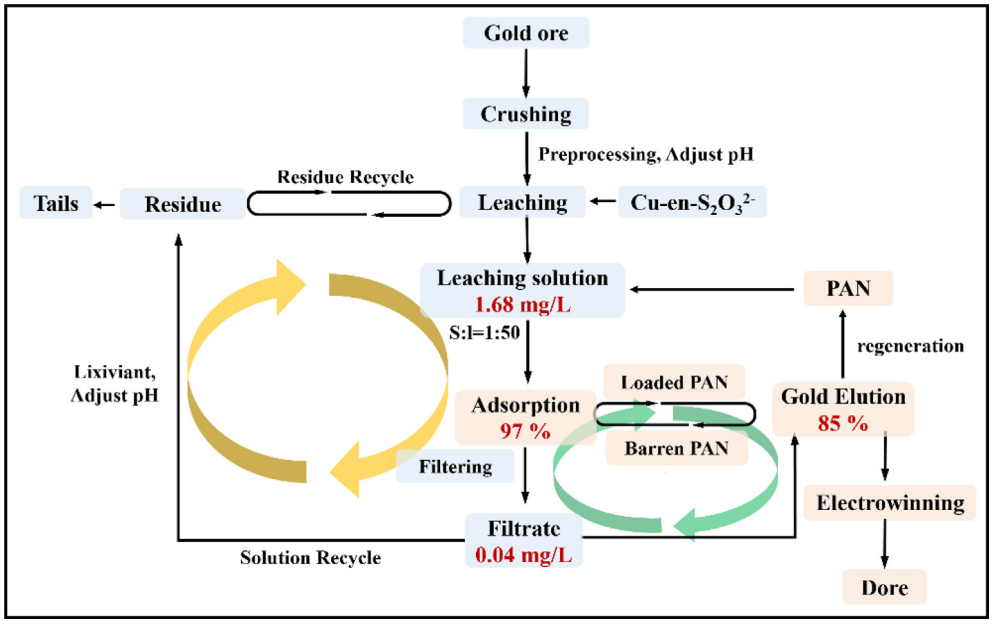

Fig. 13 Process flow chart of thiosulfate leaching and recovery.

Therefore, the adsorption mechanism of $Au(S_2O_3)_2^{3-}$ on PAN-NP can be explained to result from the combined effect of anion exchange between $H_2PO_3^-$ and $Au(S_2O_3)_2^{3-}$, complexation between Au (I) and P = O, and electrostatic attraction between $-RNH_3^+$ and $Au(S_2O_3)_2^{3-}$. Moreover, from the changes observed in the P and S elements of the EDS spectrum, it can be suggested that anion exchange could be the main mechanism. The adsorption mechanism is shown in Fig. 11.

3.4. Elution and reuse performance

The reuse performance is another important factor for evaluating the practical potential of derivatized PAN materials for gold thiosulfate leaching. For this purpose, adsorption–elution–recycle experiments were explored. An adsorption test was conducted using 0.5 g of PAN-NP using 1 mol/L of sodium sulfite as the eluent. This eluent is effectively forms PAN-NP. And the PAN-NP obtained after elution can be directly used for the next adsorption. Moreover, after five cycles of adsorption and elution, the PAN-NP still exhibits an Au (I) adsorption percentage of 61.9% (Fig. 12). Hence, There is a good reuse performance for gold thiosulfate leaching of PAN-NP.

3.5. $Au(S_2O_3)_2^{3-}$ adsorption in Cu^{2+}-en-$S_2O_3^{2-}$ system in the leaching of gold ore

The $Au(S_2O_3)_2^{3-}$ adsorption percentage obtained using PAN-NP in Cu^{2+}-en-$S_2O_3^{2-}$ systems leaching of gold ore shown in Fig. 13. The adsorption percentage of $Au(S_2O_3)_2^{3-}$ can be as high as 97% when the solid–liquid ratio is 1:50. Therefore, PAN-NP is a suitable and advantageous adsorbent for Au $(S_2O_3)_2^{3-}$ in the Cu^{2+}-en-$S_2O_3^{2-}$ system found in the actual gold ore. As the adsorption solution obtained after the completion of adsorption can be directly used in the subsequent leaching test, the adsorption solution is reusable. Hence, PAN-NP can greatly promote the recovery of $Au(S_2O_3)_2^{3-}$ in the actual leaching solution.

4. Conclusion

A novel adsorbent (PAN-NP) was prepared successfully by chemical grafting reaction and applied to recovery of $Au(S_2O_3)_2^{3-}$ from thiosulfate solution successfully. The following procedure has been implemented.

The PAN-NP prepared at 80 °C for 4 h displays a relatively satisfactory adsorption performance for $Au(S_2O_3)_2^{3-}$ which can reach 59.9%. Compared with –SH modified materials, PAN-NP has excellent qualitative properties. More importantly, the adsorption equilibrium was achieved within 20 min, which quickly, and the cumulative gold loading capacity after fifth-stage adsorption is 14.68 kg/t. The adsorption property of $Au(S_2O_3)_2^{3-}$ is affected lightly by the initial pH (5–11). Higher concentration of gold and thiosulfate have disadvantage for $Au(S_2O_3)_2^{3-}$ adsorption. the adsorption of $Au(S_2O_3)_2^{3-}$ by PAN-NP is exothermic (ΔH^0 = -9.906 kJ/mol). The adsorption behavior conform to the Langmuir adsorption model ($R^2 > 0.99$), it involves monolayer chemisorption.

Subsequently, the various properties of the adsorbent were analyzed by FT-IR, SEM, TGA, and XPS. The adsorption mechanism of $Au(S_2O_3)_2^{3-}$ by PAN-NP involves the combined effects of anion exchange $Au(S_2O_3)_2^{3-}$ with $H_2PO_3^-$, electrostatic attraction between $-RNH_3^+$ and $Au(S_2O_3)_2^{3-}$, and complexation of P = O with Au (I). PAN-NP also shows satisfactory adsorption parameters for Au $(S_2O_3)_2^{3-}$ for the Cu^{2+}-en-$S_2O_3^{2-}$ system present in the actual gold ore leaching solution (when the solid–liquid ratio is 1:50, the adsorption percentage can reach 97%). Therefore, PAN-NP is a potentially useful adsorbent for the effective adsorption of $Au(S_2O_3)_2^{3-}$ from thiosulfate solution.

CRediT authorship contribution statement

Zhujuan Li: Investigation, Methodology, Software, Formal analysis, Validation, Data curation, Visualization, Writing – original draft, Project administration, Funding acquisition.

Shuliang Chen: Data curation, Visualization, Validation, Conceptualization. **Futing Zi:** Methodology, Resources, Supervision, Writing – review & editing, Project administration, Funding acquisition. **Xianzhi Hu:** Methodology, Resources, Supervision, Writing – review & editing. **Yunlong Chen:** Investigation.

Declaration of Competing Interest

The authors declare that they have no known competing financial interests or personal relationships that could have appeared to influence the work reported in this paper.

Acknowledgements

This work was supported by the National Natural Science Foundation of China (51674128).

The authors sincerely thank the Key Laboratory of Chemical Separation Enrichment and Application in Yunnan Province Universities for their help and support.

References

Chen, S., Zi, F., Hu, X., Chen, Y., Yang, P., Wang, Q., Qin, X., Cheng, H., Liu, Y., He, Y., et al, 2020a. Interfacial properties of mercaptopropyl-functionalised silica gel and its adsorption performance in the recovery of gold (I) thiosulfate complex. Chem. Eng. J. 393, 124547.

Chen, Y., Zi, F., Hu, X., Lin, Y., Du, H., Hu, J., Yang, P., Zhang, Y., Yang, B., 2020b. The first effective utilization of activated carbon in gold thiosulfate system: A more eco-friendly, easier method for gold recovery and material regeneration. Minerals Engineering 155, 106441.

Dong, Z., Jiang, T., Xu, B., Yang, Y., Li, Q., 2017. Recovery of Gold from Pregnant Thiosulfate Solutions by the Resin Adsorption Technique. Metals 7.

Dong, Z., Jiang, T., Xu, B., Yang, Y., Li, Q., 2019. An eco-friendly and efficient process of low potential thiosulfate leaching-resin adsorption recovery for extracting gold from a roasted gold concentrate. J. Clean. Prod. 229, 387–398.

Dong, Z., Jiang, T., Xu, B., Zhang, B., Liu, G., Li, Q., Yang, Y., 2021. A systematic and comparative study of copper, nickel and cobalt-ammonia catalyzed thiosulfate processes for eco-friendly and efficient gold extraction from an oxide gold concentrate. Separation and Purification Technology 272.

Du, J., Xu, G., Lin, H., Wang, G., Tao, M., Zhang, W., 2016. Highly efficient reduction of carbonyls, azides, and benzyl halides by NaBH4 in water catalyzed by PANF-immobilized quaternary ammonium salts. Green Chem. 18, 2726–2735.

Feng, B., Yao, C., Chen, S., Luo, R., Liu, S., Tong, S., 2018. Highly efficient and selective recovery of Au (III) from a complex system by molybdenum disulfide nanoflakes. Chem. Eng. J. 350, 692–702.

Ghahremaninezhad, A., Dixon, D.G., Asselin, E., 2013. Electrochemical and XPS analysis of chalcopyrite (CuFeS2) dissolution in sulfuric acid solution. Electrochim. Acta 87, 97–112.

Grosse, A.C., Dicinoski, G.W., Shaw, M.J., Haddad, P.R., 2003. Leaching and recovery of gold using ammoniacal thiosulfate leach liquors (a review). Hydrometall. 69, 1–21.

Hiskey, J.B., Lee, J., 2003. Kinetics of gold cementation on copper in ammoniacal thiosulfate solutions. Hydrometall. 69, 45–56.

Jeon, S., Ito, M., Tabelin, C.B., Pongsumrankul, R., Kitajima, N., Park, I., Hiroyoshi, N., 2018. Gold recovery from shredder light fraction of E-waste recycling plant by flotation-ammonium thiosulfate leaching. Waste Manag. 77, 195–202.

Jeon, S., Tabelin, C.B., Takahashi, H., Park, I., Ito, M., Hiroyoshi, N., 2020. Enhanced cementation of gold via galvanic interactions using activated carbon and zero-valent aluminum: A novel approach to recover gold ions from ammonium thiosulfate medium. Hydrometall. 191.

Jiang, Y., Chen, Y., Zi, F., Hu, X., Chen, S., He, P., Zhao, L., Li, X., Li, J., Lin, Y., et al, 2022. Making untreated carbon effective in cleaner thiosulfate system: A new and high-efficiency method including gold adsorption and desorption. J. Clean. Prod. 334, 130185.

Jin Zhao, Z.W., Chen, J.-Y., 1998. Extraction of gold from thiosulfate solutions using amine mixed with neutral donor reagents. Hydrometall. 48, 133–144.

Li, G., Xiao, J., Zhang, W., 2011. Knoevenagel condensation catalyzed by a tertiary-amine functionalized polyacrylonitrile fiber. Green Chem. 13, 1828–1836.

Li, G.W., Xiao, J., Zhang, W.Q., 2012. Efficient and reusable amine-functionalized polyacrylonitrile fiber catalysts for Knoevenagel condensation in water. Green Chem. 14, 2234–2242.

Li, X., Zhang, Y., Jing, L., He, X., 2016. Novel N-doped CNTs stabilized Cu2O nanoparticles as adsorbent for enhancing removal of Malachite Green and tetrabromobisphenol A. Chem. Eng. J. 292, 326–339.

Luo, S., Li, X., Chen, L., Chen, J., Wan, Y., Liu, C., 2014. Layer-by-layer strategy for adsorption capacity fattening of endophytic bacterial biomass for highly effective removal of heavy metals. Chem. Eng. J. 239, 312–321.

Ma, T.Y., Qiao, S.Z., 2014. Acid-Base Bifunctional Periodic Mesoporous Metal Phosphonates for Synergistically and Heterogeneously Catalyzing CO2 Conversion. ACS Catal. 4, 3847–3855.

Ma, T., Zhao, R., Li, Z., Jing, X., Faheem, M., Song, J., Tian, Y., Lv, X., Shu, Q., Zhu, G., 2020. Efficient Gold Recovery from E-Waste via a Chelate-Containing Porous Aromatic Framework. ACS Appl. Mater. Interfaces 12, 30474–30482.

Nasimi, S., Baghdadi, M., Dorosti, M., 2020. Surface functionalization of recycled polyacrylonitrile fibers with ethylenediamine for highly effective adsorption of Hg (II) from contaminated waters. J. Environ. Manage. 270, 110883.

Pilśniak, M., Trochimczuk, A.W., Apostoluk, W., 2009. The Uptake of Gold (I) from Ammonia Leaching Solution by Imidazole Containing Polymeric Resins. Sep. Sci. Technol. 44, 1099–1119.

Rahaman, M.S.A., Ismail, A.F., Mustafa, A., 2007. A review of heat treatment on polyacrylonitrile fiber. Polymer Degradation and Stability 92, 1421–1432.

Ren, Z., Xu, X., Wang, X., Gao, B., Yue, Q., Song, W., Zhang, L., Wang, H., 2016. FTIR, Raman, and XPS analysis during phosphate, nitrate and Cr (VI) removal by amine cross-linking biosorbent. J. Colloid Interface Sci. 468, 313–323.

Seydibeyoğlu, M.Ö., 2012. A Novel Partially Biobased PAN-Lignin Blend as a Potential Carbon Fiber Precursor. J. Biomed. Biotechnol. 2012, 598324.

Shi, X.-L., Hu, Q., Wang, F., Zhang, W., Duan, P., 2016. Application of the polyacrylonitrile fiber as a novel support for polymer-supported copper catalysts in terminal alkyne homocoupling reactions. J. Catal. 337, 233–239.

Wang, C., Chen, S., Chen, Y., Zi, F., Hu, X., Qin, X., Zhang, Y., Yang, P., He, Y., He, P., et al, 2020. Modification of activated carbon by chemical vapour deposition through thermal decomposition of thiourea for enhanced adsorption of gold thiosulfate complex. Separation and Purification Technology 241.

Wang, Q., Hu, X., Zi, F., Yang, P., Chen, Y., Chen, S., 2019. Environmentally friendly extraction of gold from refractory concentrate using a copper – ethylenediamine – thiosulfate solution. J. Clean. Prod. 214, 860–872.

Wang, C., Wang, Z., Xu, J., Nie, Y., 2021. Analysis of Highly Efficient Adsorption of Au(S2O3)23– by Calcined Cu/Fe Layered Double Hydroxides. ACS Omega 6, 22126–22136.

Watling, K.H., Gregory A. ; Jeffrey, Matthew I. ; Woods, R. (2006). Surface Products on Gold leached in Ammoniacal Copper (II) Thiosulfate Solution. ECS Transactions *2, Issue 3, pp. 121 (2006)*, 121-132.

Wu, Y., Wang, Y., Lin, Z., Wang, Y., Li, Y., Liu, S., Gui, X., Yang, X., 2019. Three-dimensional α-Fe2O3/amino-functionalization carbon nanotube sponge for adsorption and oxidative removal of tetrabromobisphenol A. Separation and Purification Technology 211, 359–367.

Xiao, J., Wang, L., Ran, J., Zhao, J., Tao, M., Zhang, W., 2020. Highly selective removal of cationic dyes from water by acid-base regulated anionic functionalized polyacrylonitrile fiber: Fast adsorption, low detection limit, reusability. React. Funct. Polym. 146, 104394.

Xin-Gui Li, R.L., Huang, M.-R., 2005. Facile Synthesis and Highly Reactive Silver Ion Adsorption of Novel Microparticles of Sulfodiphenylamine and Diaminonaphthalene Copolymers. Chem. Mater. 17, 5411–5419.

Xin-Gui Li, M.-R.-H., Jiang, Y.-B., Zeng, J., Jie, Y.u., He, Z., 2019. Synthesis of poly (1,5-diaminonaphthalene) microparticles with abundant amino and imino groups as strong adsorbers for heavy metal ions. Microchim. Acta 186, 208.

Xin-Gui Li, M.-R.-H., Tao, T., Ren, Z., Zeng, J., Jie, Y.u., Umeyama, T., Ohara, T., Imahori, H., 2020. Highly cost-efficient sorption and desorption of mercury ions onto regenerable poly (m-phenylenediamine) microspheres with many active groups. Chem. Eng. J. 391, 123515.

Xu, B., Li, K., Li, Q., Yang, Y., Liu, X., Jiang, T., 2019. Kinetic studies of gold leaching from a gold concentrate calcine by thiosulfate with cobalt-ammonia catalysis and gold recovery by resin adsorption from its pregnant solution. Separation and Purification Technology 213, 368–377.

Xu, G., Xie, Y., Cao, J., Tao, M., Zhang, W.-Q., 2016. Highly selective and efficient chelating fiber functionalized by bis(2-pyridylmethyl) amino group for heavy metal ions11Electronic supplementary information (ESI) available. See. https://doi.org/10.1039/c6py00335d. Polymer Chemistry 7, 3874-3883.

Xu, G., Wang, L., Xie, Y., Tao, M., Zhang, W., 2018. Highly selective and efficient adsorption of Hg2+ by a recyclable aminophosphonic acid functionalized polyacrylonitrile fiber. J. Hazard. Mater. 344, 679–688.

Yang, L., Chen, J., Nie, Y., Shi, C., Wang, Q., 2021. Effective utilization of calcined MgAl-layered double hydroxides for adsorption of gold (I) thiosulfate complexes. Journal of Environmental. Chem. Eng. 9.

Yu, H., Zi, F., Hu, X., Nie, Y., Xiang, P., Xu, J., Chi, H., 2015. Adsorption of the gold–thiosulfate complex ion onto cupric ferrocyanide (CuFC)-impregnated activated carbon in aqueous solutions. Hydrometall. 154, 111–117.

Zhang, X., Li, Y., Li, M., Zheng, H., Du, Q., Li, H., Wang, Y., Wang, D., Wang, C., Sui, K., et al, 2019. Preparation of improved gluten material and its adsorption behavior for congo red from aqueous solution. J. Colloid Interface Sci. 556, 249–257.

Zhang, L., Liu, Y., Wang, Y., Li, X., Wang, Y., 2021a. Investigation of phosphate removal mechanisms by a lanthanum hydroxide adsorbent using p-XRD. FTIR and XPS. Applied Surface Science 557, 149838.

Zhang, Y., Nie, X., Dong, F., Pan, N., Ding, C., Liu, C., Wang, J., Cheng, W., Liu, M., He, H., et al, 2022. Polyamine-modified polyacrylonitrile fibers for efficient removal of U (VI) from real fluorine-contained low-level radioactive wastewater. J. Water Process Eng. 45, 102452.

Zhang, J., Pan, X., Xue, Q., He, D., Zhu, L., Guo, Q., 2017. Antifouling hydrolyzed polyacrylonitrile/graphene oxide membrane with spindle-knotted structure for highly effective separation of oil-water emulsion. Journal of Membrane Science 532, 38–46.

Zhang, Y., Xu, B., Zheng, Y., Li, Q., Yang, Y., Liu, X., Jiang, T., Lyu, X., 2021b. Hexaamminecobalt (III) catalyzed thiosulfate leaching of gold from a concentrate calcine and gold recovery from its pregnant leach solution via resin adsorption. Miner. Eng. 171.

Zhao, R., Li, X., Sun, B., Li, Y., Li, Y., Yang, R., Wang, C., 2017. Branched polyethylenimine grafted electrospun polyacrylonitrile fiber membrane: a novel and effective adsorbent for Cr (vi) remediation in wastewater. J. Mater. Chem. A 5, 1133–1144.

Zhu, H., Xu, G., Du, H., Zhang, C., Ma, N., Zhang, W., 2019. Prolinamide functionalized polyacrylonitrile fiber with tunable linker length and surface microenvironment as efficient catalyst for Knoevenagel condensation and related multicomponent tandem reactions. J. Catal. 374, 217–229.